DOI: 10.1002/anie.201209746

Enzyme Mechanism

Use of a Metallopeptide-Based Mimic Provides Evidence for a Proton-Coupled Electron-Transfer Mechanism for Superoxide Reduction by Nickel-Containing Superoxide Dismutase**

*Jason Shearer**

Superoxide ($O_2^{\bullet-}$) is a highly toxic reactive oxygen species that can induce cellular death at subnanomolar concentrations.[1] Because $O_2^{\bullet-}$ production is an unavoidable part of aerobic life, aerobic organisms have evolved superoxide detoxification systems, the most prevalent of which are the superoxide dismutases (SODs).[1,2] All known SODs have redox-active metal cofactors and detoxify superoxide through a ping-pong-type mechanism, shown in Equations 1a,b:

$$M^{red} + O_2^{\bullet-} + 2H^+ \rightarrow M^{ox} + H_2O_2 \quad (1a)$$

$$M^{ox} + O_2^{\bullet-} \rightarrow M^{red} + O_2 \quad (1b)$$

where M^{red} and M^{ox} are the reduced and oxidized forms of the metal cofactor of the metalloenzyme. The most recently discovered SOD contains nickel at its active-site (NiSOD), is found in several soil and aquatic bacteria, and operates by cycling between the reduced Ni^{II} and oxidized Ni^{III} oxidation states.[2f,3] In its reduced state, square planar Ni^{II} is ligated by two *cis*-cysteinate sulfur atoms (Cys2 and Cys6), an amidate nitrogen atom from Cys2, and the *N*-terminal amine nitrogen atom from His1 (Scheme 1).[4] Oxidation to Ni^{III} yields a square pyramidal structure by way of ligation of the His1 imidazole δ-nitrogen atom to Ni. Thus, all of the ligating residues to Ni are contained within the first six residues of the NiSOD primary sequence.

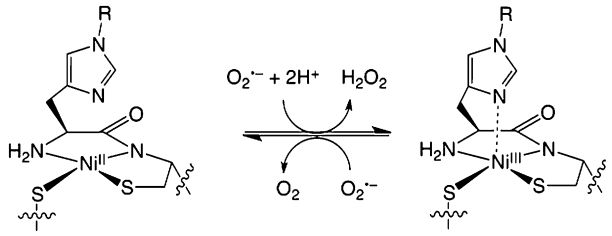

Scheme 1. NiSOD (R = H) and **Ni^{M1}** (R = CH_3) active sites.

We,[3d,5] and others,[6] have exploited this convenience of nature to generate active NiSOD biomimetics by using peptides containing the first 6–12 residues of the NiSOD sequence. Previously we demonstrated that one of these metallopeptide-based NiSOD mimics, {Ni(SOD^{M1}H(1)H^{Me})} (**Ni^{M1}**; SOD^{M1}H(1)H^{Me} = H_2N-H^{Me}CDLPCGVYDPA; H^{Me} = $^{\varepsilon}N$-methylhistidine), is isolable and stable at room temperature in both the Ni^{II} (**Ni(II)^{M1}**) and Ni^{III} (**Ni(III)^{M1}**) oxidation states.[5a] **Ni^{M1}** also performs catalytic superoxide disproportionation at a reasonably slow velocity ($k = 6(1) \times 10^6\,M^{-1}s^{-1}$; pH 8.0) making it an ideal candidate for a detailed mechanistic study.

The mechanism by which NiSOD disproportionates superoxide has not been explored in any detail, experimentally. Besides issues involving inner-sphere versus outer-sphere $O_2^{\bullet-}$ oxidation/reduction, one mechanistic point that has not been explored is the role of proton donation in the superoxide reduction half-reaction, [Eq. (1a)]. Herein, we present evidence using **Ni^{M1}** that superoxide disproportionation catalyzed by NiSOD can occur through a proton-coupled electron-transfer (PCET)-type mechanism.

First, the kinetics of superoxide disproportionation catalyzed by **Ni^{M1}** were examined using previously described stopped-flow techniques.[5a,7] The reaction was performed at pH 8.0 to suppress the $O_2^{\bullet-}$ self-disproportionation reaction.[8] At 25.0 °C, $k_{cat} = 6.1(2) \times 10^6\,M^{-1}s^{-1}$ and was in line with what was previously observed (Figure 1). Performing the reaction in D_2O (pD = 8.0)[9] resulted in a substantial solvent kinetic isotope effect (KIE); in D_2O, the $k_{cat} = 3.1(2) \times 10^5\,M^{-1}s^{-1}$, which translates into a solvent KIE of 20(4). Such a large room temperature KIE is suggestive of a PCET event with a substantial quantum-mechanical tunneling component. Under these conditions, a superoxide self-disproportionation solvent KIE of 1.2(1) was measured.

To determine if a quantum-mechanical tunneling event is a tenable hypothesis, the temperature dependence of k_{cat} on the **Ni^{M1}** catalyzed disproportionation of superoxide was examined. Rate constants were accurately determined over the temperature range of 2.0–75.0 °C. The Arrhenius plot of superoxide disproportionation is relatively flat, but still displays a slight concave appearance (Figure 2). A traditional Arrhenius analysis suggests a near barrierless reaction (activation energy of 42(4) cal mole^{-1}; pre-exponential factor of $6.45(3) \times 10^6\,s^{-1}$). These values are wholly incon-

[*] Prof. J. Shearer
Department of Chemistry
University of Nevada, Reno, NV 89557 (USA)
E-mail: shearer@unr.edu

[**] This work was supported by the National Science Foundation (CHE-0844234). X-ray absorption measurements were collected on X19a and X3b at the National Synchrotron Light Source (NSLS) which is funded by the DOE (contract no. DE-AC02-98CH10886). Work on X3b, which is part of the Case Center for Synchrotron Bioscience, was also supported by the NIH (P30-EB-009998). Profs. J. Mayer (Univ. of Washington), H. K. Shin (UNR), and an anonymous reviewer are acknowledged for valuable advice.

Supporting information for this article (experimental details) is available on the WWW under http://dx.doi.org/10.1002/anie.201209746.

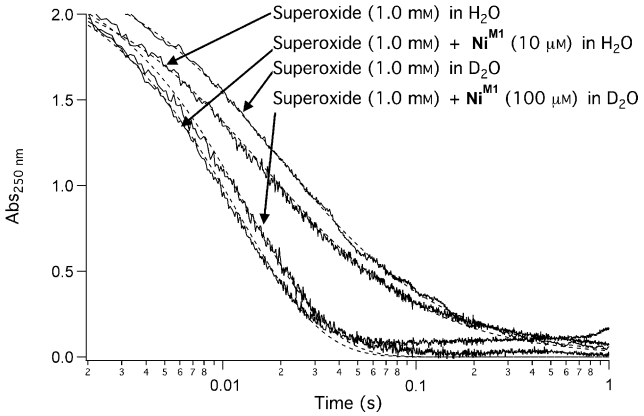

Figure 1. Superoxide decay kinetics in the presence and absence of Ni^{M1} at pH/pD 8.0 (25.0 °C). Data is represented by the solid lines and the second-order fits are represented by the dashed lines. The gradual increase in absorbance at long time lengths is related to the H_2O_2 initiated decomposition of Ni^{M1} taking place after the $O_2^{\bullet-}$ disproportionation is complete.

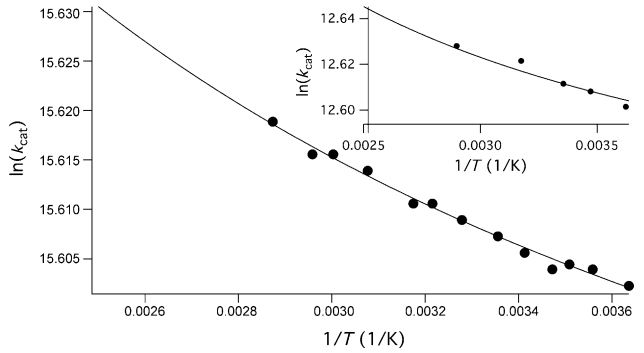

Figure 2. Arrhenius plot of Ni^{M1} catalyzed decay of superoxide at pH/pD 8.0. The main plot depicts the data collected in H_2O, the inset depicts the data collected in D_2O. Error bars are the size of the dots or smaller. The trend lines were generated using a modified Bell tunneling expression[11a] (see the Supporting Information).

sistent with estimated and measured SOD energetics.[10] The variable temperature kinetics data are consistent with SOD catalysis facilitated by Ni^{M1} that is operating by way of a tunneling mechanism.[11]

Based on the above experiments, it seems reasonable to propose that Ni^{M1} can facilitate the reduction of $O_2^{\bullet-}$ through a PCET reaction. Therefore, the reduction of **Ni(III)^{M1}** with H-atom donors possessing moderate X–H bond-dissociation free energies (BDFEs) should be possible. **Ni(III)^{M1}** was thus subjected to a series of reactions at pH 8. The reduction of **Ni(III)^{M1}** to **Ni(II)^{M1}** was achieved using ascorbate (BDFE = 73.6 kcal mole^{-1})[12] and 1-hydroxy-2,2,6,6-tetramethylpiperidine (TEMPO-H; BDFE = 71.0 kcal mole^{-1}).[12] Furthermore, **Ni(III)^{M1}** could be regenerated by adding TEMPO$^{\bullet}$ to **Ni(II)^{M1}**. In contrast, the reduction of **Ni(III)^{M1}** was not possible using reagents with slightly stronger X–H bonds, such as 1,4-dihydroquinone (first BDFE = 81.5 kcal mole^{-1})[12] and hydrazine (first BDFE = 83.4 kcal mole^{-1}).[12] This would suggest that 1) there is a hydrogen atom acceptor site within **Ni(III)^{M1}** that allows for the generation of **Ni(II)^{M1}-H** (i.e., protonated **Ni(II)^{M1}**) and 2) that the **Ni(II)^{M1}-H** BDFE is 70–80 kcal mole^{-1}.

To better estimate the **Ni(II)^{M1}-H** BDFE, an equilibrium reaction between TEMPO$^{\bullet}$/TEMPO-H and **Ni(II)^{M1}-H/Ni-(III)^{M1}** was established (Scheme 2). By varying the concentration of TEMPO$^{\bullet}$ and **Ni(II)^{M1}-H** and allowing the reaction to come to equilibrium, the equilibrium constant, K, for the reaction could be calculated. At 25.0 °C, $K = 26.5(8)$ for the **Ni(III)^{M1}** + TEMPO-H ⇌ **Ni(II)^{M1}-H** + TEMPO$^{\bullet}$ equilibrium process, which translates into a free energy of $\Delta G = -1.9(7)$ kcal mole^{-1}. A BDFE for the **Ni(II)^{M1}-H** bond of 73(1) kcal mole^{-1} can be estimated from these values. The measured BDFE is in line with the calculated BDFE based on the **Ni(II)^{M1}-H** pK_a and the previously determined redox potential of Ni^{M1} (440 mV versus a normal hydrogen electrode (NHE)).[5a] Measuring differences in the ligand-field bands of **Ni(II)^{M1}-H/Ni(II)^{M1}** as a function of pH yields a **Ni(II)^{M1}-H** pK_a of approximately 8.2. Application of a modified Bordwell equation,[12] yields a **Ni(II)^{M1}-H** BDFE of approximately 79 kcal mole^{-1}, which is in good agreement with the above measurement, considering the associated errors in the Ni^{M1} redox potential measurement.[5a] Both of these measurements are in line with the superoxide reduction process; the deprotonated product, HO_2^-, has an O–H BDFE of 81.6 kcal mole^{-1}.[12] For **Ni(II)^{M1}-H** to effectively facilitate the reduction of $O_2^{\bullet-}$ through a PCET reaction, it must have a BDFE less than the HO_2^- O–H BDFE. Otherwise the reaction would be uphill overall and not thermodynamically viable.

If there is an abstractable H atom within **Ni(II)^{M1}-H**, then there must be a well-defined protonation site near the Ni^{II} active site. An initial clue to the location of the well-defined protonation site within **Ni(II)^{M1}-H** was provided by Ni K-edge X-ray absorption spectroscopy (XAS) recorded at elevated pH. Previously, we demonstrated that at pH 7.4 **Ni(II)^{M1}-H** has an average Ni–S bond length of 2.18 Å.[5a] At pH 9.5, **Ni(II)^{M1}** has an average Ni–S bond length of 2.20 Å. This increase in bond length is consistent with a thiolate deprotonation event.[13a] Although counterintuitive, the origin of the contraction of the Ni–S bond in square planar $Ni^{II}N_2S_2$

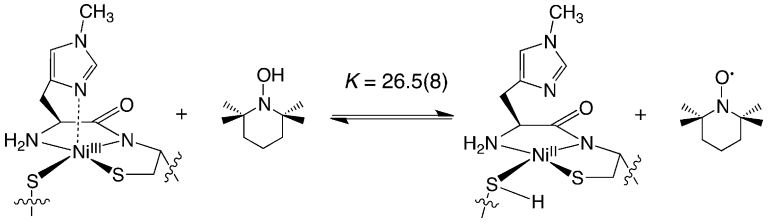

Scheme 2. Equilibrium reaction between **Ni(III)^{M1}** + TEMPO-H and **Ni(II)^{M1}-H** + TEMPO$^{\bullet}$.

complexes upon protonation or hydrogen-bond formation is well known.[13] Prontonation of the coordinated S via a filled S(p)-type lone pair reduces unfavorable filled–filled Ni(π)/S(π) interactions, leading to a bond contraction. Thus, the elongation of the Ni–S bond at high pH is consistent with cysteinate deprotonation.

A protonated Ni-S(H)-Cys bond is also consistent with room temperature S K-edge XAS performed at pH 7.4 versus 9.5. At pH 9.5, the S K-edge X-ray absorption spectrum of **Ni(II)^{M1}** is consistent with a thiolate ligated Ni^{II} complex

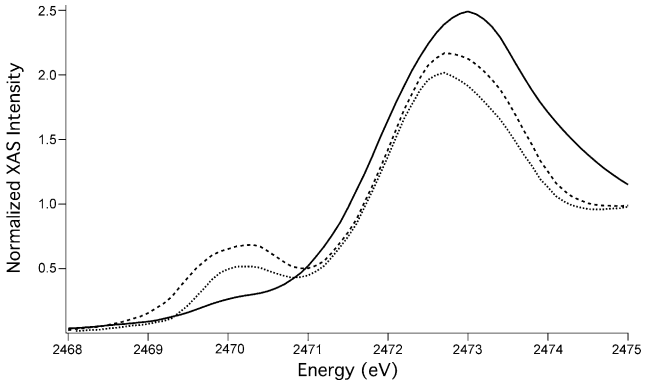

Figure 3. Sulfur K-edge XAS spectra of **Ni(II)^{M1}-H** recorded at pH 7.4 (——), **Ni(II)^{M1}** recorded at pH 9.5 (•••••), and **Ni(III)^{M1}** recorded at pH 7.4 (-----).

(Figure 3).[14] The main S(1s)→S(C-Sσ*) transition occurs at 2472.6(1) eV. Prior to the S(1s)→S(C-Sσ*) transition there is a prominent pre-edge feature corresponding to the nominal S(1s)→Ni(3d)/S(σ)* transition at 2470.4(1) eV. Similarly, the pH 7.4 S K-edge spectrum of oxidized **Ni(III)^{M1}** is consistent with a thiolate ligated Ni^{III} complex; the main S(1s)→S(C-Sσ*) transition occurs at 2473.0(1) eV while the S(1s)→Ni(3d)/S transition at approximately 2470 eV is broad, displays asymmetry, and is more intense. The change in intensity and peak shape is consistent with a) the increase in the number of holes in the Ni(3d) manifold from two to three upon oxidation and b) the fact that a lower-energy Ni(3d)/S(π)*-type orbital is now only partially filled and will accept an electron upon promotion from the S1(s) orbital. These two spectra can be contrasted with the pH 7.4 S K-edge X-ray absorption spectrum of **Ni(II)^{M1}-H**. First, there is a broadening of the main S(1s)→S(C-Sσ*) transition. Second, and more obvious, the pre-edge feature virtually disappears into the baseline. There are three conclusions that can be drawn from these results. One is that the pH 7.4 form of **Ni(II)^{M1}-H** is protonated at one (or both) of the coordinated cysteinates.[15] The second conclusion is that at pH 9.5 the coordinated cysteinate(s) becomes deprotonated. The last conclusion is that **Ni(III)^{M1}** does not contain a protonated coordinated cysteinate at low pH values.

It seems reasonable to propose that the source of the formal H-atom in reduced **Ni(II)^{M1}-H** is a protonated Ni^{II}-S(H)Cys moiety. One may expect that the pK_a of a coordinated thiolate would be rather low and inconsistent with this formulation. However, it may be that the *cis*-Cys moiety, or possibly the coordinated amine *cis* to the Cys residue, raises the pK_a of the Ni^{II}-S(H)Cys moiety higher than expected through a cooperative effect as seen in 1,8-bis(dimethylamino)naphthalene (proton sponge), for example. Other structural factors in the metallopeptide microenvironment about the Ni^{II} center may also contribute to the elevated Ni^{II}-S(H)Cys pK_a.

In summary, superoxide disproportionation catalyzed by **Ni^{M1}** was shown to occur through a rate-limiting PCET mechanism with a significant tunneling component. It appears that the PCET step occurs during the reduction of $O_2^{\bullet-}$ by protonated **Ni(II)^{M1}-H**, and the formal H-atom is in the form of a coordinated Ni^{II}-S(H)^{Cys} moiety (Scheme 3). This proposal of a PCET mechanism during superoxide reduction appears to be unique amongst the SODs, save a recent study of Cu/Zn-SOD (see below).

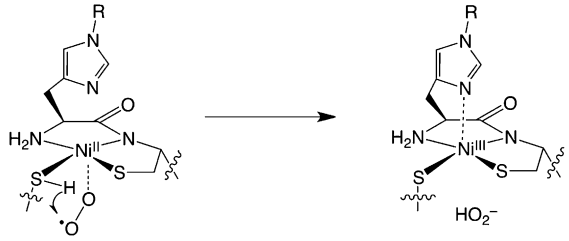

Scheme 3. Proposed mechanism of $O_2^{\bullet-}$ reduction by **Ni(II)^{M1}** and NiSOD.

Computationally, there has been one hybrid DFT study that has explicitly invoked a PCET event during the NiSOD catalyzed reduction of $O_2^{\bullet-}$.[16] In that study, the transferred "H-atom" is in the form of a Ni-S(H)-Cys moiety. The present work is consistent with the limited experimental data available concerning NiSOD itself, as well as some more recent studies on Cu/Zn SOD. First, there is strong evidence from S K-edge X-ray absorption spectroscopy that reduced NiSOD itself contains a protonated Ni^{II}-S(H)Cys moiety while the cysteinate is deprotonated upon NiSOD oxidation.[15] Second, the crystal structure of NiSOD reveals an unusual structural feature; the Ni–S bond *trans* to the amidate nitrogen is shorter than the Ni–S bond *trans* to the amine nitrogen.[4] This is the opposite of what one would expect based on the synthetic Ni^{II}N$_2$S$_2$ models with amine versus amidate coordination.[13a,b,17] It, therefore, seems reasonable to suggest that the Ni-S^{Cys} moiety *trans* to the amidate is indeed protonated in NiSOD. Analysis of the pH dependence of SOD catalysis by NiSOD itself shows that k_{cat} is pH-independent over the range of 6–8 and then falls off dramatically above pH 8.0, which is suggestive of the strong coupling of the proton-transfer event with the redox chemistry of $O_2^{\bullet-}$.[3c] Lastly, we note that at least one other SOD appears to operate through a rate-limiting proton-transfer event. A recent natural abundance $^{18}O/^{16}O$ KIE study by Roth and Smirnov provided evidence that an initial rate-limiting proton-transfer event occurs in the reduction of $O_2^{\bullet-}$ by Cu/Zn SOD under high pH conditions.[10a] In conclusion, this

study has provided insight into a possible mechanism for NiSOD, and may have relevance to other thiolate ligated metalloenzymes such as [Ni,Fe]-hydrogenase.[18]

Received: December 6, 2012
Published online: January 22, 2013

Keywords: kinetics · metalloenzymes · proton transfer · reaction mechanism · x-ray absorption spectroscopy

[1] D. M. Kurtz, Jr., *Acc. Chem. Res.* **2004**, *37*, 902 – 908.
[2] a) J. M. McCord, I. Fridovich, *J. Biol. Chem.* **1969**, *244*, 6049 – 6055; b) I. Fridovich, *Acc. Chem. Res.* **1972**, *5*, 321 – 326; c) P. J. Hart, M. M. Balbirnie, N. L. Ogihara, A. M. Nersissian, M. S. Weiss, J. S. Valentine, D. Eisenberg, *Biochemistry* **1999**, *38*, 2167 – 2178; d) K. Barnese, Y. Sheng, T. A. Stich, E. B. Gralla, R. D. Britt, D. E. Cabelli, J. S. Valentine, *J. Am. Chem. Soc.* **2010**, *132*, 12525 – 12527; e) C. K. Vance, A.-F. Miller, *Biochemistry* **1998**, *37*, 5518 – 5527; f) S. B. Choudhury, J.-W. Lee, G. Davidson, Y.-L. Yim, K. Bose, M. L. Sharma, S.-O. Kang, D. E. Cabelli, M. J. Maroney, *Biochemistry* **1999**, *38*, 3744 – 3752.
[3] a) H. D. Youn, E. J. Kim, J. H. Roe, Y. C. Hah, S. O. Kang, *Biochem. J.* **1996**, *318*, 889 – 896; b) H. D. Youn, H. Youn, J. W. Lee, Y. I. Yim, J. K. Lee, Y. C. S. O. Kang, *Arch. Biochem. Biophys.* **1996**, *334*, 341 – 348; c) B. Palenik, B. Brahamsha, F. W. Larimer, M. Land, L. Hauser, P. Chain, J. Lamerdin, W. Regala, E. E. Allen, J. McCarren, I. Paulsen, A. Dufresne, F. Partensky, E. A. Webb, J. Waterbury, *Nature* **2003**, *424*, 1037 – 1042; d) C. L. Dupont, K. Neupane, J. Shearer, B. Palenik, *Environ. Microbiol.* **2008**, *10*, 1831 – 1843.
[4] a) D. P. Barondeau, C. J. Kassmann, C. K. Bruns, J. A. Tainer, E. D. Getzoff, *Biochemistry* **2004**, *43*, 8038 – 8047; b) J. Wuerges, J.-L. Lee, Y.-I. Yim, H.-S. Yim, S.-O. Kang, K. D. Carugo, *Proc. Natl. Acad. Sci. USA* **2004**, *101*, 8569 – 8574; c) R. W. Herbst, A. Guce, P. A. Bryngelson, K. A. Higgins, K. C. Ryan, D. E. Cabelli, S. C. Garman, M. J. Maroney, *Biochemistry* **2009**, *48*, 3354 – 3369.
[5] a) J. Shearer, K. P. Neupane, P. E. Callan, *Inorg. Chem.* **2009**, *48*, 10560 – 10571; b) J. Shearer, L. Long, *Inorg. Chem.* **2006**, *45*, 2358 – 2360; c) K. P. Neupane, K. Gearty, A. Francis, J. Shearer, *J. Am. Chem. Soc.* **2007**, *129*, 14605 – 14618; d) K. P. Neupane, J. Shearer, *Inorg. Chem.* **2006**, *45*, 10552 – 10566.
[6] a) M. Schmidt, S. Zahn, M. Carella, O. Ohlenschlaeger, M. Goerlach, E. Kothe, J. Weston, *ChemBioChem* **2008**, *9*, 2135 – 2146; b) D. Tietze, H. Breitzke, D. Imhof, E. Kothe, J. Weston, G. Buntkowsky, *Chem. Eur. J.* **2009**, *15*, 517 – 523.
[7] KO_2 was solubilized in DMSO with the ether 18-crown-6 and mixed with a buffer solution of **Ni(II)^{M1}** during the stopped-flow experiment. To minimize the optical disturbance of DMSO mixing with the buffer, a final 15:1 buffer/DMSO ratio was used. D. P. Riley, W. J. Rivers, R. H. Weiss, *Anal. Biochem.* **1991**, *196*, 344 – 349.
[8] Superoxide decay kinetics catalyzed by **Ni^{M1}** recorded at pH 9.0 have rate constants of over an order of magnitude lower than those determined at pH 8.0.
[9] Note that pD values were adjusted for differences in readings from the pH meter for H_2O versus D_2O solutions and pK_a differences so $[H^+]$ and $[D^+]$ would be equal in the kinetics experiments. A. Fersht, *Structure and Mechanism in Protein Science*, W. H. Freeman and Company, New York, **1999**, p. 185.
[10] a) V. V. Smirnov, J. P. Roth, *J. Am. Chem. Soc.* **2006**, *128*, 16424 – 16425; b) A. Padiglia, R. Medda, E. Cruciani, A. Lorrai, G. Floris, *Prep. Biochem. Biotechnol.* **1996**, *26*, 135 – 142; c) M. Takahashi, K. Asada, *J. Biochem.* **1982**, *91*, 889 – 896.
[11] a) H. H. Limbach, J. M. Lopez, A. Kohen, *Philos. Trans. R. Soc. London Ser. B* **2006**, *361*, 1399 – 1415; b) Z. X. Liang, J. P. Klinman, *Curr. Opin. Struct. Biol.* **2004**, *14*, 648 – 655.
[12] J. J. Warren, T. A. Tronic, J. M. Mayer, *Chem. Rev.* **2010**, *110*, 6961 – 7001.
[13] a) C. A. Grapperhaus, M. Y. Darensbourg, *Acc. Chem. Res.* **1998**, *31*, 451 – 459; b) E. M. Gale, B. S. Narendrapurapu, A. C. Simmonett, H. F. Schaefer III, T. C. Harrop, *Inorg. Chem.* **2010**, *49*, 7080 – 7096; c) A. T. Fiedler, P. A. Bryngelson, M. J. Maroney, T. C. Brunold, *J. Am. Chem. Soc.* **2005**, *127*, 5449 – 5462; d) C. B. Allan, G. Davidson, S. B. Choudhury, Z. J. Gu, K. Bose, R. O. Day, M. J. Maroney, *Inorg. Chem.* **1998**, *37*, 4166 – 4167.
[14] T. Glaser, B. Hedman, K. O. Hodgson, E. I. Solomon, *Acc. Chem. Res.* **2000**, *33*, 859 – 868.
[15] R. K. Szilagyi, P. A. Bryngelson, M. J. Maroney, B. Hedman, K. O. Hodgson, E. I. Solomon, *J. Am. Chem. Soc.* **2004**, *126*, 3018 – 3019.
[16] V. Pelmenschikov, P. E. M. Siegnahn, *J. Am. Chem. Soc.* **2006**, *128*, 7466 – 7475.
[17] a) J. Shearer, N. Zhao, *Inorg. Chem.* **2006**, *45*, 9637 – 9639; b) H.-J. Krüger, G. Peng, R. H. Holm, *Inorg. Chem.* **1991**, *30*, 734 – 742.
[18] K. Weber, T. Krämer, H. Shafaat, T. Weyhermüller, E. Bill, M. van Gastel, F. Neese, W. Lubitz, *J. Am. Chem. Soc.* **2012**, *134*, 20745 – 20755.

